Journal of Marine Systems 139 (2014) 241–247

Contents lists available at ScienceDirect

Journal of Marine Systems

journal homepage: www.elsevier.com/locate/jmarsys

Influence of continental shelf processes in the water mass balance and productivity from stable isotope data on the Southeastern Brazilian coast

Igor M. Venancio [a], Andre L. Belem [a], Tarcio Henrique R. dos Santos [b], Maria do R. Zucchi [b], Antonio Expedito G. Azevedo [b], Ramsés Capilla [c], Ana Luiza S. Albuquerque [a,*]

[a] Departamento de Geoquímica, Universidade Federal Fluminense, Outeiro de São João Batista, s/nº., Niterói, Rio de Janeiro CEP: 24020-141, Brazil
[b] Universidade Federal da Bahia, Instituto de Física, Departamento de Geofísica Nuclear, Rua Caetano Moura, 123, 40210-350 Salvador, BA, Brazil
[c] CENPES-Petrobras/Geoquímica Network, Cidade Universitária, Ilha do Fundão, RJ 21941-915, Brazil

ARTICLE INFO

Article history:
Received 15 October 2013
Received in revised form 10 June 2014
Accepted 17 June 2014
Available online 24 June 2014

Keywords:
Stable isotopes
Mixing processes
Water masses
Upwelling
Southeastern Brazilian continental shelf

ABSTRACT

Stable isotopic composition ($\delta^{18}O$ and δD of water, $\delta^{13}C_{DIC}$) of the water column in the open ocean is related to the origin of water masses. Due to the recent increase of paleoceanographic studies on continental shelves, it is also important to understand their distribution and variability in those systems. To examine the influence of continental shelves internal processes on isotopic composition of water masses, we present data of stable isotopes and phosphate content from a western boundary upwelling system located on the Southeastern Brazilian coast and compare them with offshore observations. High mixing of the main water masses (SSW, TW and SACW) was observed in the majority of the samples collected during different seasons in 2011 and 2012. A mixing triangle approach was used to separate the water masses contribution and characterize their isotopic composition. In addition, an isotopic three end-member model was established, proposing it as a paleoceanographic tool to reconstruct relative contribution of these water masses in sediment records. Variations of $\delta^{18}O$ values are linked to oceanographic dynamics, mixing, continental runoff and upwelling processes on the shelf. Differently the $\delta^{13}C_{DIC}$ variations in the middle and inner parts of the shelf are related to the productivity of the upwelling system. Seasonal variability of the $\delta^{13}C_{DIC}$ values may be also related to changes in the upwelling intensity.

1. Introduction

The oceans are an important redistribution agent for the constituents of the Earth's climate system, as heat, fresh water and carbon dioxide. Variations of these constituents affect the climate and leave imprints that can be tracked by geochemical tracers. One of these tracers is the isotopic composition of water masses. The relevance of this specific tracer lies on the fact that biogenic carbonate is assumed to be in isotopic equilibrium with water. As a consequence isotopic composition of foraminifera has been one of the most widely used tools to reconstruct both the variations in sea surface temperature and salinity ($\delta^{18}O$) and paleoproductivity ($\delta^{13}C$) in marine cores (Ganssen et al, 2011; Morley et al, 2011; Piotrowski et al, 2009; Thornalley et al, 2010). The establishment of isotopic equilibrium functions, based on culture experiments (Bemis et al, 1998; Erez and Luz, 1983; Kim and O'Neil, 1997) and calibrated by studies with tops cores (Grauel and Bernasconi, 2010; Steph et al, 2009), trawled plankton nets (Mulitza et al, 2003) and sediment traps (Sautter and Thunell, 1991; Wejnert et al, 2010), make possible to reconstruct the variations of temperature (SST) and salinity (SSS) in sea surface water in paleoceanographic studies. However, the accuracy of these SST–SSS reconstructions still depends primarily on assumed values for the $\delta^{18}O$ of seawater, which despite being considered conservative and near the standard VSMOW (Vienna Standard Mean Ocean Water) for the open ocean, can suffer large variations on the continental margins resulting from the action of oceanic and shelf water mixing including continental water contribution, the balance of precipitation–evaporation (P:E) which is distinct between west and east ocean boundaries, or even coastal upwelling, bypassing thus the average signal of global scale (Bigg and Rohling, 2000; Mackensen, 2001; Meredith et al, 1999).

Moreover, searching high resolution records, especially for the Holocene, many studies have used marine sediments deposited on the continental shelf (Limmer et al, 2012; Mendes et al, 2010; Nizou et al, 2011) whose dynamics results from interactions of shelf processes such as mixing, continental runoff and coastal upwelling, and the mesoscale boundary processes, which contains much of the climatic oscillations of the boundary currents. Under these conditions the oxygen isotopic composition of seawater ($\delta^{18}Ow$) deviates from the values of open ocean waters, and imprints significantly the oxygen isotopic composition of the carbonate ($\delta^{18}Oc$) used to reconstruct paleotemperatures of calcification. Therefore, an assessment of the degree of mixing of

* Corresponding author at: Departamento de Geoquímica, Universidade Federal Fluminense, Outeiro São João Batista, s/n, Centro, Niterói, Rio de Janeiro CEP 24020-150, Brazil. Tel.: +55 21 26292197; fax: +55 21 26292234.
E-mail address: ana_albuquerque@id.uff.br (A.L.S. Albuquerque).

http://dx.doi.org/10.1016/j.jmarsys.2014.06.009
0924-7963/

the shelf waters is critical to propose accurate paleotemperature reconstructions based on the oxygen isotopic composition of carbonate shells of foraminifers of sediments from the continental shelf.

Continental margins also represent the main productive compartment of the oceans. The potential fertilization of coastal waters arising from runoff and aeolian inputs and from upwelling of deeper and colder nutrient rich waters alters the carbon isotopic composition of the dissolved inorganic carbon ($\delta^{13}C_{DIC}$), which is recorded in the $\delta^{13}C$ values of biogenic carbonates, thus influencing, the understanding of the variance of paleoproductivity signal (Eberwein and Mackensen, 2008; Lückge et al, 2009). This is especially valid on the western boundary of the oceans where the signal of local upwelling systems may vary significantly from the paleoproductivity of boundary current waters (Bickert and Wefer, 1999).

On the Southwestern Atlantic, the only study that addresses the isotopic composition of seawater was conducted by Pierre et al. (1991), that through the pair $\delta^{13}C_{DIC}$ and $\delta^{18}Ow$ showed a clear distinction between the main water masses carried by the main Western Boundary Current, the Brazil Current: TW (Tropical Water), SACW (South Atlantic Central Water), and the waters on intermediate depths carried by less organized deep currents AAIW (Antarctic Intermediate Water), NADW (North Atlantic Deep Water) and AABW (Antarctic Bottom Water). However, the oceanographic regime of the open ocean is distinct from the continental shelf, which can lead to differences in the isotopic composition of the water masses of the Brazil Current (TW and SACW). Albuquerque et al (2014) and Belem et al (2013) showed that, in the Eastern Brazilian Continental Shelf (EBS), multiple oceanographic processes act together to control shelf temperature variability near the shelf break and inshore of the western boundary current, and the isotopic composition of these shelf water masses will thus reflect in part these processes. Starting from these pioneering results, this study aims to understand how the typical processes of dynamic shelf influence the isotopic compositions ($\delta^{18}Ow$, δ Dw and $\delta^{13}C_{DIC}$) of water masses of the Brazil Current and the EBS to improve the accuracy of paleoceanographic reconstructions from sedimentary cores of the continental shelf.

2. Oceanographic setting

The continental shelf of southeastern Brazil, especially between the parallels 21°S and 25°S (Fig. 1), is widely studied due to the upwelling system in the area of Cabo Frio (e.g. Castelao, 2012; Castelao and Barth, 2006; Castro and Miranda, 1998; Ikeda et al., 1974; Matsuura, 1996; Rodrigues and Lorenzzetti, 2001; Diaz et al, 2012). The Brazil Current (BC) flows southward along the shelf break and slope, as a component of South Atlantic Subtropical Gyre and gains integrity and velocity south of Abrolhos bank (Campos et al., 2000). However, around 23°S the continental margin changes orientation from NE–SW sharply to E–W. Instability in the BC flow associated with prevailing NE trade winds and a wind divergent on the midshelf (Castelao and Barth, 2006) causes an enhanced pumping of SACW on the shelf and the formation of an Upwelling System which controls the local oceanography and production in the area (Belem et al, 2013). Moreover, this boundary current carries the Tropical Water (TW) in the upper layer and the South Atlantic Central Water (SACW) in a more intermediate depth southward (Stramma and England, 1999). The TW and the SACW, additionally to the Coastal Water (CW), are the main water masses in this region (Castro and Miranda, 1998).

These three different water masses are characterized by their temperature and salinity patterns (Fig. 1). The TW is associated with temperatures higher than 20 °C and salinities above 36.4. The CW and TW have the same temperature range but the CW is characterized by lower salinities than the TW, as a result from the mixing of shelf waters and continental drainage (Castro and Miranda, 1998) although the contribution of river discharge is minor (Oliveira et al, 2006). However some studies also define the CW as Subtropical Shelf Water (SSW) (Piola et al, 2000) and we decided to adopt the term SSW in this study. Finally, the presence of SACW on the shelf is characterized by temperatures below 20 °C and salinities lower than those of TW (Castro and Miranda, 1998; Silveira et al., 2000). The SACW can be found at the surface near the coast characterizing the costal upwelling of Cabo Frio that is most associated with the persistence of intense NE winds and is also explained by bottom topography, coastline geometry and wind stress curl (Castelao and Barth, 2006; Rodrigues and Lorenzzetti, 2001). In the inner shelf, upwelling is enhanced during austral spring and summer and is seasonally modulated by NE winds (Cerda and Castro, 2013). However in the mid-shelf, Belem et al. (2013) and Albuquerque et al. (2014) pointed out that SACW intrusions in the euphotic zone (sub-surface upwelling) are intermittent all over the year. This Western Boundary Upwelling System (WBUS) is considered unique due to its configuration in a mosaic of oceanographic systems, which acts synergetically in biogeochemical processes on the shelf (Albuquerque et al, 2014). Typically, the region is defined as oligotrophic due to the TW characteristics but with enhanced local productivity due to the upwelling.

We emphasize that, although the SACW outcrops at the surface in the coastal region, producing an upwelling in its sensu strict definition, it

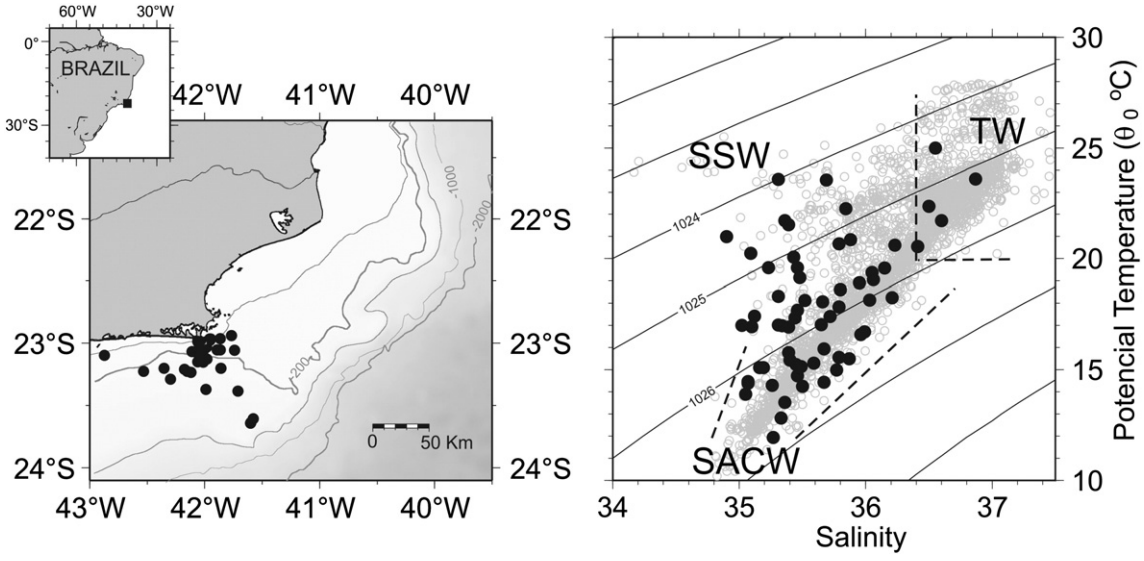

Fig. 1. Location of oceanographic stations and regional T–S diagram. The gray dots represent T–S extracted from NODC database for the region and the black dots represent the data collected in this study.

Table 1
Oceanographic data.

Cruise	Station	Date/Hour	Longitude	Latitude	Depth (m)	Temperature (°C)	Salinity (psu)	$\delta^{18}O$ (‰)	$\delta^{13}C_{DIC}$ (‰)	δD (‰)	Phosphate (μmol/l)	SACW [%]	TW [%]	SSW [%]
WH11-01	WH11-01#01	2011-03-25T06:52:58	−41.5788	−23.6059	50.02	23.59	36.87	0.98	1.90	8.90		20.32	72.74	6.94
WH11-01	WH11-01#01	2011-03-25T07:04:00	−41.5984	−23.6370	81.68	20.61	36.23	0.97	1.30	8.20		38.07	48.86	13.07
WH11-01	WH11-01#02	2011-03-25T10:17:00	−41.7111	−23.3853	52.12	19.05	36.06	0.65	1.71	7.10		48.07	41.36	10.57
WH11-01	WH11-01#03	2011-03-25T12:34:00	−41.8583	−23.2013	49.29	18.14	36.03	0.64	1.84	6.70		54.20	39.08	6.72
WH11-01	WH11-01#04	2011-03-25T14:38:00	−41.9828	−23.0321	49.36	15.14	35.49	0.62	1.85	6.10		72.51	18.20	9.29
WH11-01	WH11-01#02	2011-03-25T10:19:00	−41.7105	−23.3847	98.12	14.73	35.46	0.54	1.52	5.50		75.20	16.67	8.12
WH11-01	WH11-01#04	2011-03-25T14:41:00	−41.9885	−23.0341	82.80	14.25	35.50	0.46	1.38	5.20		78.68	17.16	4.16
WH11-01	WH11-01#03	2011-03-25T12:38:00	−41.8583	−23.2013	91.29	13.52	35.36	0.57	1.57	6.10		83.10	11.82	5.08
WH11-02	WH11-02#01	2011-05-27T10:53:00	−42.0613	−23.1498	45.13	15.55	35.79	0.67	1.55	6.10		62.97	33.49	3.54
WH11-02	WH11-02#01	2011-05-27T10:56:00	−42.0613	−23.1498	90.71	14.43	35.67	0.53	1.28	5.40		70.13	28.18	1.69
WH11-03	WH11-03#03	2011-07-14T13:12:00	−41.9899	−23.3722	25.35	21.53	35.39	0.39	2.70	4.60		21.01	31.16	47.83
WH11-03	WH11-03#02	2011-07-14T09:47:00	−42.0121	−23.1535	23.63	20.99	34.90	0.18	2.60	3.90		22.91	15.87	61.22
WH11-03	WH11-03#02	2011-07-14T09:49:00	−42.0121	−23.1535	80.44	18.31	35.31	0.19	2.30	3.80		42.54	23.71	33.75
WH11-03	WH11-03#01	2011-07-14T07:10:00	−42.0309	−23.0142	23.34	17.42	35.12	0.53	0.92	2.93		47.89	16.70	35.40
WH11-03	WH11-03#03	2011-07-14T13:15:00	−41.9899	−23.3722	86.60	17.02	35.31	0.32	2.20	4.10		51.28	21.67	27.05
WH11-03	WH11-03#01	2011-07-14T07:13:00	−42.0309	−23.0142	63.72	16.94	35.10	0.05	1.90	3.20		51.07	15.36	33.57
WH12-01	WH12-01#02	2012-03-09T13:06:30	−41.8911	−23.0538	16.21	20.55	36.41	0.60	1.80	4.70	0.142	39.25	54.23	6.52
WH12-01	WH12-01#1B	2012-03-09T10:50:00	−41.9565	−22.9649	17.03	18.61	35.80	0.26	2.06	3.97	0.061	49.97	32.82	17.21
WH12-01	WH12-01#02	2012-03-09T15:43:20	−41.8911	−23.0538	36.38	18.25	36.21	0.61	1.44	2.56	0.948	54.21	44.70	1.08
WH12-01	WH12-01#1A	2012-03-09T09:40:05	−41.9565	−22.9649	18.59	17.84	35.79	0.08	2.43	3.10		55.23	31.36	13.42
WH12-01	WH12-01#01	2012-03-09T11:02:10	−41.9565	−22.9649	26.52	17.68	35.46	0.20	2.17	3.59	0.075	54.91	21.11	23.98
WH12-02	WH12-02#03	2012-04-03T11:43:15	−41.7395	−23.0561	7.02	23.58	35.31	0.26	2.02	2.43	0.09	6.83	32.04	61.12
WH12-02	WH12-02#02	2012-04-03T15:03:25	−41.8656	−23.0529	4.72	23.55	35.69	0.22	2.18	1.03	0.08	8.40	43.19	48.41
WH12-02	WH12-02#01	2012-04-03T17:05:00	−42.0093	−23.0561	8.97	20.66	35.79	0.26	2.01	1.50	0.264	28.34	41.57	30.09
WH12-02	WH12-02#03	2012-04-03T10:50:00	−41.7395	−23.0561	35.64	19.15	35.48	0.32	1.81	2.07	0.231	37.46	30.05	32.49
WH12-02	WH12-02#02	2012-04-03T14:39:05	−41.8656	−23.0529	60.29	15.49	35.87	0.36	1.86	1.97	0.259	63.66	35.75	0.59
WH12-02	WH12-02#01	2012-04-03T16:53:00	−42.0093	−23.0561	53.82	14.98	35.77	0.03	1.16	0.84	0.901	66.76	32.00	1.24
WH12-03	WH12-03#2B	2012-05-29T11:24:35	−42.1211	−23.2350	1.21	21.72	35.36	0.55	1.87	3.92		19.62	30.57	49.81
WH12-03	WH12-03#01	2012-05-29T08:38:15	−42.1772	−23.2092	5.09	20.23	35.09	0.26	2.04	1.63	0.183	28.74	20.26	50.99
WH12-03	WH12-03#03	2012-05-29T13:36:25	−42.1517	−23.2278	11.87	20.06	35.43	0.58	1.81	1.25	0.256	31.12	30.01	38.87
WH12-03	WH12-03#02	2012-05-29T11:09:26	−42.1211	−23.2350	8.89	19.59	35.23	0.37	2.02	2.49	0.224	33.58	23.38	43.04
WH12-03	WH12-03#03	2012-05-29T14:10:05	−42.1117	−23.0667	42.18	16.93	35.39	0.61	1.25	3.31	0.53	52.18	23.89	23.93
WH12-03	WH12-03#02	2012-05-29T11:36:00	−42.2981	−23.2908	40.85	15.10	35.16	0.42	1.21	0.68	0.808	63.75	14.21	22.03
WH12-03	WH12-03#01	2012-05-29T09:57:10	−42.3536	−23.2006	42.57	14.46	35.07	0.26	1.16	2.46	0.808	67.77	10.55	21.68
WH12-05	WH12-05#03	2012-08-22T08:56:50	−41.9797	−23.1272	13.18	22.26	35.84	0.52	1.55	3.41	0.234	17.68	45.57	36.75
WH12-05	WH12-05#02	2012-08-22T11:18:00	−42.0545	−23.0736	9.96	19.58	36.15	0.62	1.44	2.89	0.308	36.96	50.47	12.58
WH12-05	WH12-05#03	2012-08-22T09:24:00	−41.9948	−23.1290	47.85	16.71	35.99	0.64	1.19	2.78	0.447	55.83	41.22	2.96
WH12-05	WH12-05#02	2012-08-22T11:56:00	−42.0803	−23.0715	34.17	16.59	35.96	0.44	1.01	2.71	0.516	56.53	40.14	3.32
WH12-05	WH12-05#01	2012-08-22T13:57:00	−42.0619	−22.9843	6.23	12.81	35.33	0.41	1.19	1.97	0.298	79.88	15.60	4.51
WH12-05	WH12-05#01	2012-08-22T14:42:10	−42.0619	−22.9843	29.65	11.94	35.27	0.29	1.06	1.60	1.062	85.56	12.46	1.98
WH12-06	WH12-06#01	2012-09-21T06:39:20	−41.9533	−22.9780	8.91	19.59	35.46	0.63	1.62	3.18	0.144	34.41	30.15	35.44
WH12-06	WH12-06#02	2012-09-21T08:31:10	−42.0007	−23.0308	6.85	17.34	35.44	0.65	1.54	3.54	0.273	49.58	26.01	24.41
WH12-06	WH12-06#01	2012-09-21T07:32:00	−41.9760	−22.9859	34.88	15.44	35.40	0.47	1.01	2.49	0.695	62.31	21.82	15.86
WH12-06	WH12-06#03	2012-09-21T11:44:00	−42.0411	−22.9878	6.78	17.00	35.02	0.40	1.36	2.73	0.457	50.38	13.09	36.53
WH12-06	WH12-06#03	2012-09-21T12:16:00	−42.0411	−22.9878	17.38	14.39	35.07					68.24	10.44	21.32
WH12-06	WH12-06#02	2012-09-21T09:13:48	−42.0212	−23.0400	34.64	13.89	35.05	0.38	1.26	2.40	0.938	71.63	9.04	19.33
WH12-08	WH12-08#03	2012-10-30T10:02:00	−41.7674	−22.9377	11.35	20.86	35.88	0.53	1.63	2.34	0.098	27.31	44.54	28.15
WH12-08	WH12-08#02	2012-10-30T13:35:00	−41.8658	−22.9621	11.22	18.07	35.66	0.48	1.04	3.34	0.533	45.43	33.64	20.93
WH12-08	WH12-08#01	2012-10-30T15:37:00	−41.9479	−22.9666	11.36	17.04	35.65	0.42	0.88	1.40	0.626	52.37	31.72	15.91
WH12-08	WH12-08#01	2012-10-30T15:55:00	−41.9479	−22.9666	36.67	15.23	35.45	0.42	1.14	2.57	0.794	63.92	22.97	13.12
WH12-08	WH12-08#03	2012-10-30T11:06:00	−41.7674	−22.9377	49.59	15.94	35.67	0.43	1.15	3.81	0.724	59.90	30.57	9.53
WH12-08	WH12-08#02	2012-10-30T12:53:00	−41.8658	−22.9621	44.60	15.29	35.59	0.40	1.13	3.40	0.883	64.01	27.19	8.80
WH12-09	WH12-09#03	2012-12-13T09:19:00	−42.0193	−23.1042	17.22	22.35	36.50	0.65	1.22	5.24		27.26	59.66	13.08
WH12-09	WH12-09#02	2012-12-13T12:06:00	−42.0456	−23.0466	10.52	18.92	35.95	0.65	1.19	2.10		48.49	37.83	13.68
WH12-09	WH12-09#03	2012-12-13T09:53:00	−42.0193	−23.1042	28.49	19.37	36.05	0.45	0.85	4.37		45.82	41.54	12.64
WH12-09	WH12-09#02	2012-12-13T11:21:00	−42.0456	−23.0466	24.39	17.40	35.72	0.60	0.99	1.96		57.95	28.57	13.47
WH12-09	WH12-09#01	2012-12-13T14:37:00	−42.0556	−22.9955	10.96	16.99	35.34	0.32	1.43	3.15		59.14	16.44	24.42
WH12-09	WH12-09#01	2012-12-13T13:59:00	−42.0556	−22.9955	26.60	14.30	35.26	0.47	1.07	2.95		77.37	9.95	12.68
WHx12-01	WHx12-01#01	2012-05-10T15:40:02	−41.6026	−23.6413	10.56	24.99	36.55	0.89	1.85	2.83	0.105	1.74	70.81	27.46
WHx12-01	WHx12-01#01	2012-05-10T16:03:10	−41.6026	−23.6413	80.10	15.09	35.19	0.85	1.05	6.80	0.598	63.93	15.08	20.99
WHx12-02	WHx12-02#03	2012-09-03T21:51:19	−42.5308	−23.2263	1.61	21.72	36.60	0.76	1.46	4.98	0.070	24.07	67.11	8.82
WHx12-02	WHx12-02#02	2012-08-27T15:50:30	−42.8728	−23.0964	1.05	18.13	35.52	0.38		0.71	0.204	44.52	29.61	25.87
WHx12-02	WHx12-02#01	2012-08-27T13:11:58	−43.1239	−22.9665	1.25	15.77	35.39	0.27	1.82	2.35	0.501	60.04	22.05	17.91

occurs only in a range of a few miles from the coast, i.e. the coastal Ekman area. However, other important mechanisms in the mid- and outer shelf are marked by constant intrusions of SACW in the photic zone (Belem et al, 2013; Castelao and Barth, 2006), which does not fit the classic definition adopted of upwelling, but produces significant effects on productivity and biogeochemical processes in this region, with pronounced impact on the isotopic composition of shelf water masses.

3. Material and methods

3.1. Sampling strategy

Between March 2011 and December 2012 a total of thirty two stations were sampled in 12 cruises on the Southeastern Brazilian Shelf that were performed by two vessels, the navy ship “Aspirante Moura” and the research trawler “PL Divers” (Fig. 1). Temperature and salinity

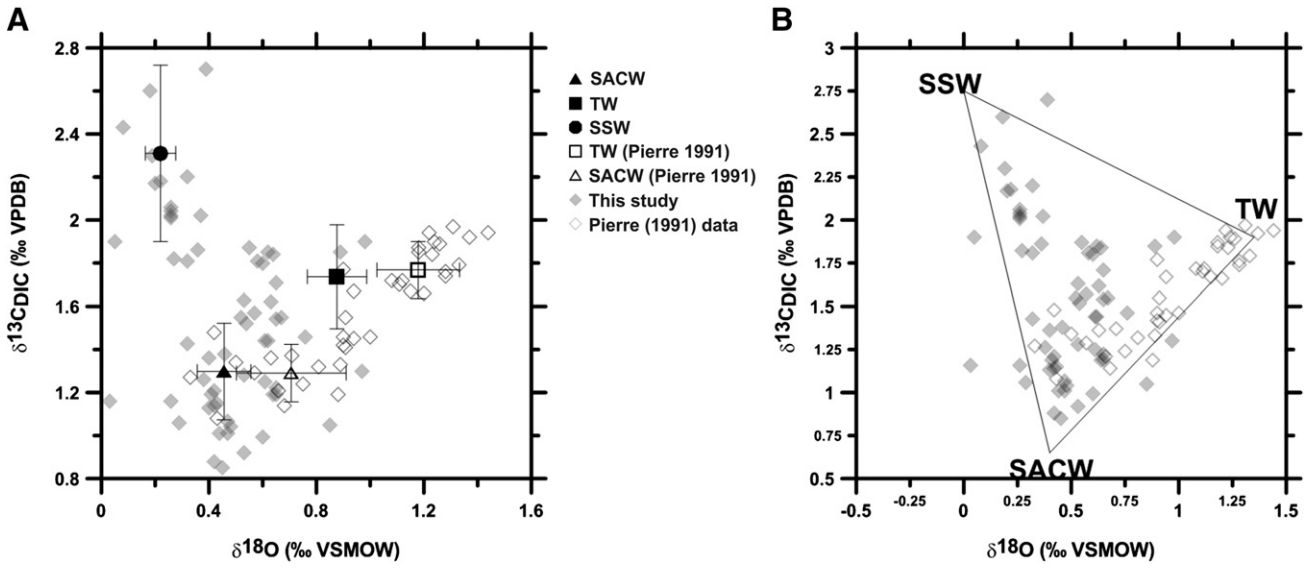

Fig. 2. Stable isotopic composition of each water mass and the three end-member model. (a) $\delta^{18}O$–$\delta^{13}C_{DIC}$ plot after the mixing triangle analysis, including Pierre et al. (1991). (b) 3 end-member based $\delta^{18}O$ and $\delta^{13}C_{DIC}$ for each water mass.

profile data were obtained with a multiparameter YSI 6600V2 sonde. After identifying the water masses by their TS pairs, water samples were taken from specific depths using a 5 L Niskin bottle coupled with the secondary YSI 6600V2 sonde mounted in a frame. A total of sixty three discrete samples were collected and analyzed (Table 1).Samples for stable isotope analysis were stored in 100 mL amber vials and fixed with 1 ml of a saturated mercuric chloride solution. For phosphate analysis we separated sub-samples of 1 L, and dissolved (<0.45 μm, filtered in GF/F filters) phosphate ion was determined by spectrophotometry (Grasshoff et al., 1999).

3.2. Technical procedures

Each water sample was analyzed for dissolved inorganic carbon (DIC), oxygen and hydrogen stable isotopes of water. Abundances were reported in δ notation in parts per thousand:

$$\delta = (R\ sample/R\ reference - 1)\ x\ 1000$$

The $\delta^{13}C_{DIC}$ analyses were performed with an IRMS (Isotope Ratio Mass Spectrometer) and international standard VPDB (Vienna Pee Dee Belemnite) was used as reference. Subsamples of 700 μL were placed in vials containing 30 μL of phosphoric acid. These subsamples were pressurized with helium gas to release carbon dioxide (McCrea, 1950). After 18 h at 25 °C, the released CO_2 was sent to the IRMS (ThermoFinnigan MAT Delta ^{PLUS}) through an open-split interface of Finnigan II Gas Bench that manages the input and reference gas samples as well as their injection and dilution in the spectrometer. The analysis is replicated and the average values are calculated among 10 peaks analyzed for all samples and standards. The isotopic value for $\delta^{13}C_{DIC}$ is reported in relation to the primary reference VPDB. The accuracy of the measurement is 0.1‰.

For $\delta^{18}O$ and δD analyses we used a CRDS (Cavity Ring-Down Spectrometer) (Berden and Engeln, 2009) and the primary reference was the VSMOW (Vienna Standard Mean Ocean Water). The experimental apparatus consists of a Laser System (Model L2120-I Picarro) containing a resonant cavity ring-down type. Thus, 2 μL aliquots of water are injected into a vaporizer at 110 °C to produce water vapor that is sent to the analyzer along with a carrier gas N_2. Each measurement is based on the decay time of the intensity of the light beam, enabling to determine the absorption coefficient and measure isotopic hydrogen and oxygen ratios simultaneously. In CDRS, the δ value can be calculated from the measured absorption coefficient αn where n refers to the lighter isotope – more abundant ($y = H^{16}OH$) and heavier – less abundant ($x = H^{18}OH$, $H^{17}OH$ or $H^{16}OD$) respectively.

$$\delta(x) = \frac{R_x^{sample}}{R_x^{references}} - 1 = \frac{\left(a_x/a_y\right)^{sample}}{\left(a_x/a_y\right)^{reference}} - 1 = \frac{\left(a_x^{sample}/a_x^{reference}\right)}{\left(a_y^{sample}/a_y^{reference}\right)} - 1$$

Each sample was measured 8 times, the first 3 were discarded due to memory effect. The $\delta^{18}O$ and δD values were calculated in relation to the primary standards of the International Atomic Energy Agency (IAEA): VSMOW, SLAP and GISP. The accuracy of measurement is 0.3‰ for δD and 0.05‰ to $\delta^{18}O$. These measurements were performed at the Lab of Nuclear Physics, Department of Physics of the Earth and the Environment, Federal University of Bahia.

Table 2
Termohaline coefficients and isotopic end-members for water masses types.

WATER MASS	Termohaline Coefficients		Observed		Adopted	
	Temperature	Salinity	^{13}C	^{18}O	^{13}C	^{18}O
SSW	24[a]/25[b]	34.2[a]/34.4[b]	2.31(0.41)	0.22 (0.06)	2.75	0
TW	25.75[a]/27[b]	37.5[a]/37.6[b]	1.74 (0.24)	0.88 (0.11)	1.9	1.35
SACW	9.65[a]/10.9[b]	34.97[a]/35.1[b]	1.30 (0.22)	0.46 (0.10)	0.65	0.4

[a] Values for winter condition (May–October).
[b] Values for summer condition (November–April).

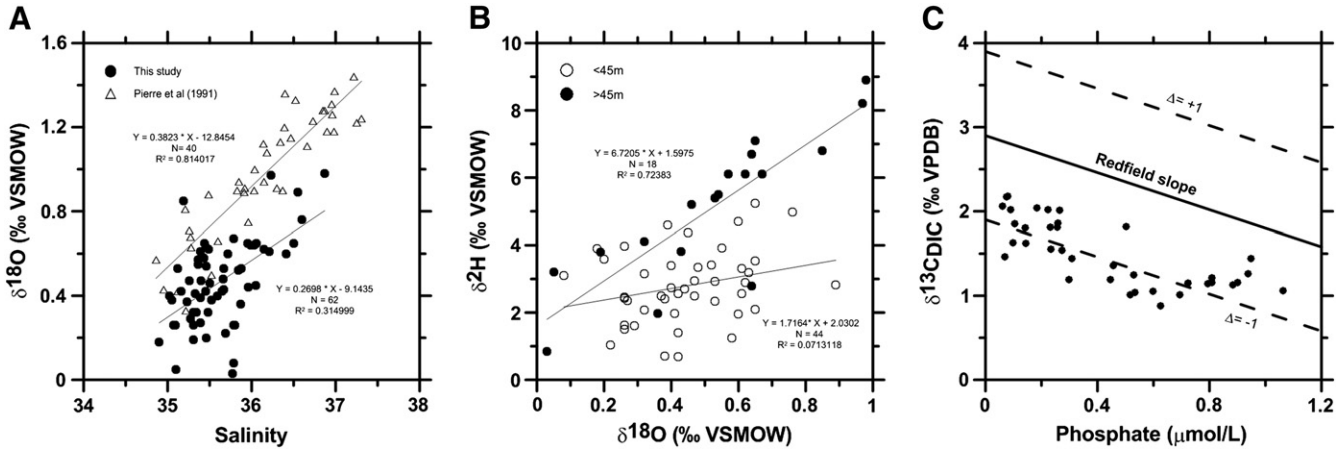

Fig. 3. Plots indicating internal processes on the shelf. (a) $\delta^{18}O$-salinity plot of Pierre et al. (1991) data and this study data. (b) $\delta^{18}O$–δD plot below and above 45 m with linear regression and correlation coefficients. (c) $\delta^{13}C_{DIC}$-phosphate data. The solid line represents the biological fractionation trend and the dashed lines represent the thermodynamic shifts from biologic trend (Broecker and Maier-Reimer, 1992).

4. Results and discussion

Hydrographic data as well as isotopic values for each sample are summarized in Table 1. From temperature and salinity pairs of each sample, it was possible to estimate the relative contribution of the main water masses. For this purpose, we used the classic method of mixing triangle (Pickard and Emery, 1990) assuming that each water mass in the study area has specific thermohaline coefficients and allowing the calculation of proportions of each water type for individual samples (Castro et al, 1998). The thermohaline coefficients applied here were defined from a set of points of historical oceanographic stations of the World Ocean Database for the region and the TS index of each water type was divided by a summer and by a winter set. Between November and April, the pairs of SSW (T = 25.5; S = 34.4), TW (T = 27; S = 37.6) and SACW (T = 10.9; S = 35.1) were established for the continental shelf. From May to October, the mean values of SSW (T = 24; S = 34.2), TW (T = 25.75; S = 37.5) and SACW (T = 9.65; S = 34.97) were slightly different.

The proportions obtained from the mixing triangle analysis (Table 1) show that the majority of the samples collected on the continental shelf have a high degree of mixing. This was expected since the continental shelf is a very dynamic and complex system with multiple factors influencing the physical structure of the water column like, continental runoff, coastal upwelling and the mid-shelf upwelling driven by wind stress curl. Samples with more than 60% of contribution from a particular water mass were chosen to calculate the mean and standard deviation of their isotopic characteristics (Fig. 2a). These values were then compared with the study of Pierre et al. (1991), which surveyed some of these water masses in an offshore region. Our isotopic data for the TW ($\delta^{18}O = 0.88 \pm 0.11$; $\delta^{13}C_{DIC} = 1.74 \pm 0.24$) and SACW ($\delta^{18}O = 0.46 \pm 0.10$; $\delta^{13}C_{DIC} = 1.30 \pm 0.22$) on the shelf are quite similar from those found offshore, with a slight deviation for the $\delta^{18}O$ toward lower values, suggesting that internal processes from the continental shelf can influence the $\delta^{18}O$ values of those water masses, as expected. In our understanding this deviation is possibly caused by two distinct factors. One is the mixing triangle approach itself, because since no

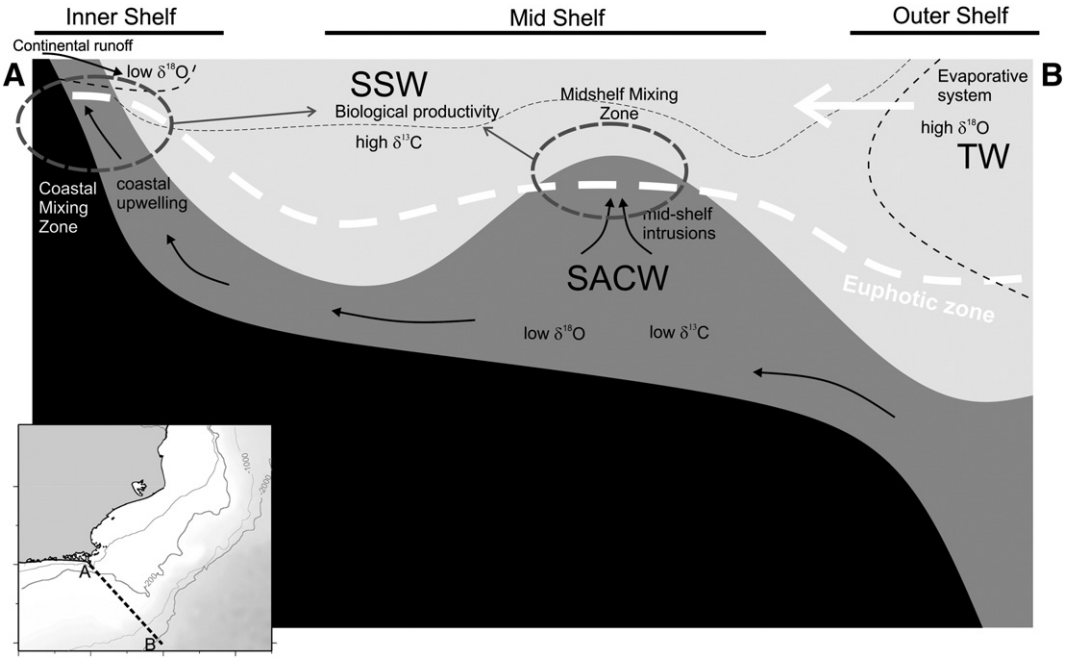

Fig. 4. Conceptual model based on oceanographic settings and distribution of stable isotopes on the shelf of a western boundary current system.

sample was found with >90% of contribution of a singular water mass type, residual contribution from other water masses remains in each sample. This shift can be attributed to processes on the shelf that lower $\delta^{18}O$ values. In that case, the deviation could be linked to continental runoff that brings fresh water depleted in ^{18}O or to mixing with a large contribution of the SSW, which carries water with lower $\delta^{18}O$ values. Although we cannot rule out the influence of the evaporation-precipitation balance for the TW entering the shelf where the increasing influence of precipitation might contribute also to lower the $\delta^{18}O$ values (Craig and Gordon, 1965; Gat et al, 1996).

For SSW ($\delta^{18}O = 0.22 \pm 0.06$; $\delta^{13}C_{DIC} = 2.31 \pm 0.41$) there are no values available for comparison. However, the $\delta^{13}C_{DIC}$ values found for this water mass indicate large ^{13}C enrichment. Considering that the main factors influencing the $\delta^{13}C_{DIC}$ are the thermodynamic and biological fractionations, we tried to found the dominant factor by considering the amplitude of the deviation. The 1‰ difference of the $\delta^{13}C_{DIC}$ values of SSW and TW, cannot be explained by the thermodynamic effect as the main factor since according to Broecker and Maier-Reimer (1992) such variation would represent at least 10 °C difference between TW and SSW, which was never observed in any previous data (Belem et al, 2013; Castelao and Barth, 2006). Conversely, this shift could be attributed to biological isotopic fractionation from high productivity triggered by SACW intrusions in the euphotic zone, either by coastal Ekman transport caused by northeast winds or by wind-stress-curl driven upwelling (Castelao and Barth, 2006). Therefore, these specific oceanographic events drive the fertilization of the euphotic zone, promoting consumption of nutrients by enhanced primary production and the preferential use of ^{12}C-rich DIC by phytoplankton (Charles et al, 1993; Kroopnick, 1985).

Based in these results a three end-member water masses can be defined with their characteristic isotopic ($\delta^{18}O$–$\delta^{13}C$) values (Fig. 2b, Table 2). This approach will allow to characterize the structure of the water column and to further estimate the relative contribution of each water mass in past conditions, using the isotopic records of foraminifers (Mackensen, 2001).

In addition to their paleoceanographic interest, stable isotopes of present day ocean waters support the understanding of modern oceanographic dynamics and biogeochemical processes active in the water column. Analyzing the $\delta^{18}O$, δD and $\delta^{13}C_{DIC}$ behaviors with physical parameters, some of these processes were evidenced. The relation between $\delta^{18}O$ and salinity suggested a different correlation on the shelf, when compared with offshore condition described by Pierre et al (1991) (Fig. 3a). The high offshore correlation can be attributed to a well-defined vertical TS structure of the water column. In contrast, the continental shelf under strong lateral and vertical mixing does not show the same pattern. Continental discharge and coastal upwelling may contribute to mixing and a poor correlation between $\delta^{18}O$ and salinity. Another important aspect is the influence of multiple sources with different $\delta^{18}O$ signatures, but not necessarily with different salinity values, which is a possible explanation for the observed trend (Meredith et al, 1999). This is evidenced by the large range of $\delta^{18}O$ values in waters with salinity between 35 and 36. Furthermore, $\delta^{18}O$ values are lower on the shelf, when compared with offshore, indicating influence of coastal plumes, as well as the mixing of SSW with other water masses, which are internal processes able to lower the mean $\delta^{18}O$ signal on the shelf.

To estimate the influence of vertical mixing on the shelf the relation δD–$\delta^{18}O$ was plotted (Fig. 3b). In general, these isotopes are linearly correlated in the open ocean, since the same fractionation mechanisms are affecting both elements (Craig and Gordon, 1965). However, under a shallow and variable water column structure, deviations from this general trend are expected and data showed distinct relations relative to the depth of the sample. A threshold limit of 45 m was chosen after testing the change of the correlation along the depth gradient. Above this depth, δD and $\delta^{18}O$ presented a non-conservative behavior, indicating that the structure of the water column is not stable with a high degree of mixing. Below 45 m depth, a conservative behavior between these isotopes was found, resulting probably from conservative mixing between SACW and TW. The works of Cerda and Castro (2013) and Castro (2013) have shown that the average mixing layer depth is 45–50 m in Cabo Frio, which corroborates with our findings. These results confirm the idea of a complex oceanographic scenario on the shelf, but also improve our knowledge, since it gives us a vertical dimension of the influence of mixing processes.

Finally, to confirm the hypothesis of $\delta^{13}C_{DIC}$ in the water column being modulated mainly by biological productivity, a good correlation with phosphate was found. Fig. 3c shows the relation between $\delta^{13}C_{DIC}$ and phosphate, compared with the "Redfield line" proposed by Broecker and Maier-Reimer (1992). The same approach was made in other upwelling systems to verify the magnitude of biological processes in the $\delta^{13}C_{DIC}$ variability (Bickert and Wefer, 1999) and our results confirms the dominance of fractionation due to biological productivity, demonstrating that $\delta^{13}C_{DIC}$ in the water column reflects productivity on the shelf. Seasonal changes in the upwelling activity may also cause variations in the $\delta^{13}C_{DIC}$ values. Nevertheless, the lack of points for some months and the sampling design do not allow a definitive conclusion about the seasonality of the data. This result allows one to make possible paleoproductivity reconstructions on the shelf, or to reconstruct the potential fertility of the SACW using $\delta^{13}C$ from benthic foraminifers. We also expect that future interpretations based on the $\delta^{13}C$ of the carbonate of these organisms should take into account the differences between the shelf and open ocean systems relative to $\delta^{13}C_{DIC}$ signal in the water column, which is extremely important as shown by previous studies (Bickert and Wefer, 1999; Pierre et al, 1994).

Coupling our understanding of the regional physical oceanography and interpretations of stable isotope variations, a conceptual model of functioning of the continental shelf is proposed (Fig. 4). The model shows that oscillations of the BC and consequently improved relative contribution of the TW, carry waters with high $\delta^{18}O$ values on outer and middle shelf. In the case of SSW and SACW, the oxygen isotopic compositions are lower and the influence of the SSW is more restricted to the inner and middle shelf, whereas SACW can influence the whole water column. Higher $\delta^{13}C_{DIC}$ are found in the inner and middle shelf, where the upward movements of SACW (upwelling and sub-surface intrusion of SACW) promote higher productivity and imprint this signal to the SSW. In the outer part, the oligotrophic TW maintains the $\delta^{13}C_{DIC}$ levels stable and close to its own $\delta^{13}C_{DIC}$ signature.

5. Conclusions

The continental shelf of the Southeastern Brazilian coast is submitted to the influence of different water sources. There is a significant variability of $\delta^{18}O$ and δD comprised in a short salinity interval that is linked to inputs of different sources of waters on the continental shelf (e.g. coastal plumes). The influence of these plumes, as other surface processes (upwelling), seems to be the main driven mechanism of vertical changes in correlation between δD and $\delta^{18}O$. In contrast, the $\delta^{13}C_{DIC}$ deviations were less expressive for TW and SACW characterized on the shelf. The $\delta^{13}C_{DIC}$ values for the SSW and the correlation between $\delta^{13}C_{DIC}$ and phosphate indicate the major imprint of biological cycling, with a possible seasonal variability demonstrating the magnitude of productivity in this upwelling system and focusing attention for the potential of paleoproductivity proxies on the shelf.

6. Acknowledgments

This study was financially supported by the Geochemistry Network from PETROBRAS/National Petroleum Agency (ANP) of Brazil (Grant 0050.004388.08.9). A.L.S. Albuquerque are senior scholars from CNPq (National Council for the Development of Science and Technology, Brazil, Grant 306385/2013-9). We are grateful to the anonymous reviewers for their constructive comments that greatly contributed in improving the manuscript.

References

Albuquerque, A.L.S., Belem, A.L., Zuluaga, F.J.B., Cordeiro, L.G.M., Mendoza, U., Knoppers, B., Gurgel, M.H.C., Meyers, P.A., Capilla, R., 2014. Particle fluxes and bulk geochemical characterization of the Cabo Frio upwelling system in Southeastern Brazil: sediment trap experiments between Spring 2010 and Summer 2012. An. Acad. Bras. Cienc. 86 (2) 601-619.

Belem, A.L., Castelao, R.M., Albuquerque, A.L.S., 2013. Controls of subsurface temperature variability in a western boundary upwelling system. Geophys. Res. Lett 40, 1366. http://dx.doi.org/10.1002/grl.50297.

Bemis, B.E., Spero, H.J., Bijma, J., Lea, D.W., 1998. Reevaluation of the oxygen isotopic composition of planktonic foraminifera: experimental results and revised paleotemperature equations. Paleoceanography 13, 150–160.

Berden, G., Engeln, R., 2009. Cavity ring-down spectroscopy: techniques and applications, ed. Wiley, United Kingdom.

Bickert, T., Wefer, G., 1999. South Atlantic and benthic foraminifer δ13C deviations: implications for reconstructing the late quaternary deep-water circulation. Deep-Sea Res. II 46, 437–452.

Bigg, G.R., Rohling, E.J., 2000. An oxygen isotope data set for marine waters. J. Geophys. Res. 105 (C4), 8527–8536.

Broecker, W.S., Maier-Reimer, E., 1992. The influence of air and sea exchange on the carbon isotope distribution in the sea. Glob. Biogeochem. 6 (3), 315–320.

Campos, E.J.D., Velhote, D., Silveira, I.C.A., 2000. Shelf break upwelling driven by Brazil current cyclonic meanders. Geophys. Res. Lett. 27, 751–754.

Castelao, R.M., 2012. Sea surface temperature and wind stress curl variability near a cape. J. Phys. Oceanogr. 42, 2073–2087. http://dx.doi.org/10.1175/JPO-D-11-0224.1.

Castelao, M.R., Barth, J.A., 2006. Upwelling around Cabo Frio, Brazil: the importance of wind stress curl. Geophys. Res. Lett. 33. http://dx.doi.org/10.1029/2005GL025182 (L03602).

Castro, B.M., 2013. Summer/winter stratification variability in the central part of the South Brazil Bight. Cont. Shelf Res. http://dx.doi.org/10.1016/j.csr.2013.12.002.

Castro, B.M., Miranda, L.B., 1998. Physical oceanography of the western Atlantic continental shelf located between 4°N and 34°S. In: Robinson, A.R., Brink, K.H. (Eds.), The Sea. 11. John Wiley, Hoboken, N. J, pp. 209–251.

Castro, C.G., Pérez, F.F., Holley, S.E., Ríos, A.F., 1998. Chemical characterization and modeling of water masses in the Northeast Atlantic. Prog. Oceanogr. 41, 249–279.

Cerda, C., Castro, B.M., 2013. Hydrographic climatology of South Brazil Bight shelf waters between Sao Sebastiao (24°S) and Cabo Sao Tome (22°S). Cont. Shelf Res. http://dx.doi.org/10.1016/j.csr.2013.11.003i.

Charles, C.D., Wright, J.D., Fairbanks, R.G., 1993. Thermodynamic influences on the marine carbon isotope record. Paleoceanography 8, 691–697.

Craig, H., Gordon, L.I., 1965. Deuterium and oxygen-18 variations in the ocean and the marine atmosphere. In: Tongiorgi, E. (Ed.), Stable isotopes in oceanographic studies and paleotemperatures. Spoleto, Italy, pp. 9–130.

Diaz, R., Moreira, M., Mendoza, U., Machado, W., Bottcher, M.E., Santos, H., Belem, A., Capilla, R., Escher, P., Albuquerque, A.L., 2012. Early diagenesis of sulfur in a tropical upwelling system, Cabo Frio, Southeastern Brazil. Geologija 40, 879–882. http://dx.doi.org/10.1130/G33111.1.

Eberwein, A., Mackensen, A., 2008. Last glacial maximum paleoproductivity and water masses off NW-Africa: evidence from benthic foraminifera and stable isotopes. Mar. Micropaleontol. 67, 87–103.

Erez, J., Luz, B., 1983. Experimental paleotemperature equation for planktonic foraminifera. Geochim. Cosmochim. 47, 1025–1031.

Ganssen, G.M., Peeters, F.J.C., Metcalfe, B., Anand, P., Jung, S.J.A., Kroon, D., Brummer, G.-J. A., 2011. Quantifying sea surface temperature ranges of the Arabian Sea for the past 20, 000 years. Clim. Past 7, 1337–1349.

Gat, J.R., Shemesh, A., Tziperman, E., Hecht, A., Georgopoulos, D., Basturk, O., 1996. The stable isotope composition of waters of the eastern Mediterranean Sea. J. Geophys. Res. 101, 6441–6451.

Grasshoff, K., Kremling, K., Ehrhardt, M., 1999. Methods of seawater analysis, 3rd ed. Wiley-VCH, New York, Chichester, Brisbane, Singapore, Toronto, Weinheim (634p).

Grauel, A.L., Bernasconi, S.M., 2010. Core-top calibration of δ18O and δ13C of G. ruber (white) and U. Mediterranea along the southern Adriatic coast of Italy. Mar. Micropaleontol. 77, 175–186.

Ikeda, Y., Miranda, L.B., Miniussi, I.C., 1974. Observations on stages of upwelling in the region of Cabo Frio (Brazil) as conducted by continuous surface temperature and salinity measurements. Bol. Inst. Oceanogr. 23, 33–46.

Kim, S.-T., O'Neil, J.R., 1997. Equilibrium and nonequilibrium oxygen isotope effects in synthetic carbonates. Geochim. Cosmochim. 61, 3461–3475.

Kroopnick, P.M., 1985. The distribution of ^{13}C of ΣCO: in the world oceans. Deep-Sea Res. 32, 57–84.

Limmer, D.R., Boning, P., Giosan, L., Ponton, C., Kohler, C.M., Cooper, M.J., Tabrez, A.R., Clift, P.D., 2012. Geochemical record of Holocene to recent sedimentation on the Western Indus continental shelf, Arabian Sea. Geochem. Geophys. Geosyst. 13 Q01008.

Lückge, A., Mohtadi, M., Rühlemann, C., Scheeder, G., Vink, A., Reinhardt, L., Wiedicke, M., 2009. Monsoon versus ocean circulation controls on paleoenvironmental conditions off southern Sumatra during the past 300,000 years. Paleoceanography 24 PA1208.

Mackensen, A., 2001. Oxygen and carbon stable isotope tracers of Weddell Sea water masses: new data and some paleoceanographicimplications. Deep-Sea Res. I 48, 1401–1422.

Matsuura, Y., 1996. A probable cause of recruitment failure of Brazilian Sardine (*Sardinella aurita*) population during the 1974/75 spawning season. S. Afr. J. Mar. Sci. 17, 29–35.

McCrea, J.M., 1950. On the isotopic chemistry of carbonates and a paleotemperature scale. J. Chem. Phys. 18, 849–857.

Mendes, I., Rosa, F., Dias, J.A., Schonfeld, J., Ferreira, Ó., Pinheiro, J., 2010. Inner shelf paleoenvironmental evolution as a function of land–ocean interactions in the vicinity of the Guadiana River, SW Iberia. Quat. Int. 221, 58–67.

Meredith, M.P., Grose, K.E., McDonagh, E.L., Heywood, K.J., Frew, R.D., Dennis, P., 1999. The distribution of oxygen isotopes in the water masses of Drake Passage and the South Atlantic. J. Geophys. Res. 104 (20), 949–962.

Morley, A., Schulz, M., Rosenthal, Y., Mulitza, S., Paul, A., Ruhlemann, C., 2011. Solar modulation of North Atlantic central water formation at multidecadal timescales during the late Holocene. Earth Planet. Sci. Lett. 308, 161–171.

Mulitza, S., Boltovskoy, D., Donner, B., Meggers, H., Paul, A., Wefer, G., 2003. Temperature: δ18O relationships of planktonic foraminifera collected from surface waters. Paleogeogr. Paleoclimatol. Paleoecol. 202, 143–152.

Nizou, J., Hanebuth, T.J.J., Vogt, C., 2011. Deciphering signals of late Holocene fluvial and aeolian supply from a shelf sediment depocentre off Senegal (north-west Africa). J. Quat. Sci. 26, 411–421.

Oliveira, J., Charette, M., Allen, M., Braga, E.S., Furtado, V.V., 2006. Coastal water exchange rate studies at the southeastern Brazilian margin using Ra isotopes as tracers, Radioact. Environ. 8, 345-359. http://dx.doi.org/10.1016/S1569-4860(05)08028-9.

Pickard, G.L., Emery, W.J., 1990. Descriptive physical oceanography, An introduction, 5th EditionButterworth-Heinemann Ltd, Geat Britain.

Pierre, C., Vergnaud-Grazzini, C., Faugères, J.C., 1991. Oxygen and carbon stable isotope tracers of the water masses in the Central Brazil Basin. Deep-Sea Res. 38 (5), 597–606.

Pierre, C., Vangriesheim, A., Laube-Lenfant, E., 1994. Variability of water masses and of organic production-regeneration systems as related to eutrophic, mesotrophic an oligotrophic conditions in the northeast Atlantic Ocean. J. Mar. Syst. 5, 159–170.

Piola, A.R., Campos, E.J.D., Moller, O.O., Charo, M., Martinez, C., 2000. Subtropical shelf front off eastern South America. J. Geophys. Res. 105, 6565–6578.

Piotrowski, A.M., Banakar, V.K., Scrivner, A.E., Elderfield, H., Galy, A., Dennis, A., 2009. Indian Ocean circulation and productivity during the last glacial cycle. Earth Planet. Sci. Lett. 285, 179–189.

Rodrigues, R.R., Lorenzzetti, J.A., 2001. An numerical study of the effects of bottom topography and coast line geometry on the southeast Brazilian coastal upwelling. Cont. Shelf Res. 21, 371–394.

Sautter, L.R., Thunell, R.C., 1991. Planktonic foraminiferal response to upwelling and seasonal hydrographic conditions; sediment trap results from San Pedro Basin, Southern California Bight. J. Foraminifer. Res. 21, 347–363.

Silveira, I.C.A., Schmidt, A.C.K., Campos, E.J.D., Godoi, S.S., Ikeda, Y., 2000. The Brazil current off the eastern Brazilian Coast. Rev. Bras. Oceanogr. 48 (2), 171–183.

Steph, S., Regenberg, M., Tiedemann, R., Mulitza, S., Nurnberg, D., 2009. Stable isotopes of planktonic foraminifera from tropical Atlantic/Caribbean core-tops: implications for reconstructing upper ocean stratification. Mar. Micropaleontol. 71, 1–19.

Stramma, L., England, M., 1999. On the water masses and mean circulation of the South Atlantic Ocean. J. Geophys. Res. 104 (C9), 20863–20883.

Thornalley, D.J.R., Elderfield, H., McCave, I.N., 2010. Intermediate and deep water paleoceanography of the northern North Atlantic over the past 21,000 years. Paleoceanography 25 PA1211.

Wejnert, K.E., Pride, C.J., Thunell, R.C., 2010. The oxygen isotope composition of planktonic foraminifera from the Guaymas Basin, Gulf of California: seasonal, annual, and interspecies variability. Mar. Micropaleontol. 74, 29–37.